Journal of Water Process Engineering 37 (2020) 101504

Contents lists available at ScienceDirect

Journal of Water Process Engineering

journal homepage: www.elsevier.com/locate/jwpe

Hydrothermal synthesis of TiO_2 nanoflower deposited on bauxite hollow fibre membrane for boosting photocatalysis of bisphenol A

Nurul Jannah Ismail[a], Mohd Hafiz Dzarfan Othman[a,*], Suraini Abu Bakar[b], Siti Hamimah Sheikh Abdul Kadir[c], Mohd Haiqal Abd Aziz[a], Mohd Arif Budiman Pauzan[a], Siti Khadijah Hubadillah[a], Tijjani El-badawy[a], Juhana Jaafar[a], Mukhlis A Rahman[a]

[a] Advanced Membrane Technology Research Centre (AMTEC), School of Chemical and Energy Engineering, Universiti Teknologi Malaysia, 81310, Skudai, Johor, Malaysia
[b] Pusat Penyelidikan Nanoteknologi, Fakulti Sains dan Matematik, Universiti Pendidikan Sultan Idris, 35900 Tanjung Malim, Perak, Malaysia
[c] Institute of Medical Molecular Biotechnology, Faculty of Medicine, Sungai Buloh Campus, Universiti Teknologi MARA (UiTM), Jalan Hospital, 47000 Sungai Buloh, Selangor, Malaysia

ARTICLE INFO

Keywords:
TiO_2 nanoflower
Photocatalyst
Bisphenol A
Ceramic membrane
Bauxite

ABSTRACT

The special physical and chemical properties of titanium dioxide (TiO_2), including the environmental friendliness and facile fabrication, have made it the most widely studied photocatalyst. The use of TiO_2 largely relies on its morphological traits, crystal structure, and phase dimension. The uniqueness of TiO_2nanoflower structure with a coarse texture and arranged structures demonstrates higher photocatalytic activity for organic pollutants. A simple hydrothermal synthesis was used in this study with TiO_2 nanoflowers implanted on the surface of bauxite-based hollow fibre membrane (BHFM). The modification was done to enhance the photocatalytic performance of the BHFM as this membrane naturally possesses catalytic property. The decorated BHFM was then subjected to catalytic degradation of bisphenol A (BPA) under irradiation of UV light. The synthesis of TiO_2 nanostructure on the membrane surface was successfully performed based on SEM images, and it has good water permeability of 323.76, 309.32 and 280.42 L/h.m^2.bar for 2.5 h, 5.0 h and 7.5 h of hydrothermal time respectively. A significant difference of 25 % between the modified and unmodified BHFM was notable, which indicates its potential as a new material for photocatalyst. As a conclusion, the modified BHFM possessed enhanced photocatalytic properties under both UV light and visible light.

1. Introduction

The technology on photocatalyst or semiconductors has been studied with excellent findings. The unique properties of TiO_2, which is inexpensive, high stability, harmlessness, bioinert materials, reduction–oxidation ability, and biodegradability makes it a potential photocatalyst in the degradation of pollutants in the water system [1]. Moreover, TiO_2 nanomaterials are used extensively in the form of nanopowder, nanowires, nanotubes, nanoflowers, and nanoparticles [2]. In terms of catalytic performance, nanoflowers possess a large surface area, and their thickness is the lowest compared to others. Those properties attract considerable attention due to their incredible performance [3]. The benefit of having a large surface area makes the materials to produce a high photocatalytic efficiency for photocatalytic activity on the surface

TiO_2 is available in three types of structural form, namely rutile, anatase, and brookite [4]. Due to its high photoactivity, inexpensive, high stability, and negative potential for conduction band, anatase structure has been potrayed as the most effective photocatalyst [5]. The characteristic of anatase structure of TiO_2 that encompasses redox properties and high stability has made it widely nominated as photocatalyst [6] and other applications including solar cells [7], water and air purification, and self-cleaning of antibacterial materials [8]. The presence of high-density surface hydroxyl groups slows down the recombination of photogenerated charge carriers. The highly specific surface area and anatase crystallinity greatly influence the photocatalytic performance of TiO_2.

Bauxite contains aluminium oxide (alumina) with various degrees of hydration (amorphous aluminium oxide dihydrate is $Al_2O_3{\cdot}2H_2O$), varying in colour from white to brown, and is dull in appearance. Bauxite contains a small amount of natural anatase (TiO_2) which is a well-known semiconductor [9]. The red colouration of the bauxite is due to the presence of mineral named hematite which is also recognised as ferric oxide (Fe_2O_3) indicating the quality and utility of the bauxite

* Corresponding author.
E-mail address: hafiz@petroleum.utm.my (M.H.D. Othman).

https://doi.org/10.1016/j.jwpe.2020.101504
Received 1 July 2020; Accepted 4 July 2020

[10]. This iron compound (α-Fe_2O_3) has a band gap of around 2.1 eV which gains increasing interest as it is cost effective, highly stable, readily available, non-poisonous, and is known as having visible light-responsive characteristic [11]. Unfortunately, coupling α-Fe_2O_3 to semiconductor TiO_2 has rarely been recorded. Li et al. [12] developed the branch-shaped nanocomposites of α-Fe_2O_3/TiO_2 through combination of electrospinning and hydrothermal methods. In the same study, they reported that for organic dyes and methylene blue (MB) degradation, the usage of nanocomposites displayed outstanding result on visible-light photocatalytic activities in visible light spectrum due to its large surface area of 42.8 m^2/g, a continuous visible-light absorption, and improved photogenerated charge separation. By using bauxite as it contains TiO_2 and Fe_2O_3, the chances to produce coupling α-Fe_2O_3–TiO_2 semiconductor with unknown performance is possible.

Bauxite is beneficial for several applications particularly water treatment including removal of phenols [13], heavy metals [14], nitrates [15], phosphates [16], and dye coloured wastewater [17]. Bauxite is effective for removing recalcitrant organic contaminants. Thus, in this study, fabricated bauxite hollow fibre membrane underwent surface modification by implementing TiO_2 nanomaterial through the hydrothermal method to boost the photocatalytic property of the membrane for the removal of a type of endocrine disruptor compound (EDC) known as bisphenol A (BPA).

2. Experimental Procedures

2.1. Materials

Sieved bauxite powder of 50 μm (Aras Kuasa Sdn. Bhd.), *N*-methyl-2-pyrrolidone (NMP, AR grade, Merck), polyethersulfone (PES, Solvay Advanced Polymers), and Arlacel P135 (Uniqema) were used as the ceramic particle, solvent, binder, and dispersant, respectively. During the process of ceramic extrusion, tap water was used as both internal and coagulation medium. Similarly, step-wise increase of concentrated hydrochloric acid (HCl) from 36.5%–38%, deionised water, and titanium tetrabutoxide (TBOT) were used for the hydrothermal reaction. Degradation of contaminant under the UV radiation was conducted using BPA as the organic contaminant representing EDC.

2.2. Laboratory work

BHFM (50 wt%) was produced by homogenously mixing bauxite powder, solvent (NMP, 42.75 wt%), polymer binder (PES, 6.25 wt%), and dispersant (Arlacel P135, 1 wt%) to yield a bauxite suspension. The degassed suspension was then ready to be extruded through phase inversion technique with a flow rate of 9 mL/min for the suspension and 10 mL /min for internal coagulant via tube-in-orifice spinneret (ID 1.2 mm, OD 2.8 mm) directly into the external coagulant bath with 5 cm air gap. Subsequently, BHFM precursor was submerged approximately 24 h in the external coagulation bath to complete the phase inversion process before drying at room temperature. All BHFM precursors underwent the sintering process in a tubular furnaceat1300 ˚C (Magna value, XL-1700) applying the same sintering profile from previous work [18]. The sintered BHFM was ready for further modifications.

For the surface modification of BHFM with titanium dioxide (TiO_2), concentrated hydrochloride acid (HCl) was mixed into deionised water at a ratio of 1:1 and stirred vigorously using a glass rod for about 10 min. Titanium tetrabutoxide (TBOT, 6 mL) was then added drop-wise into the solution and stirred until the solution turned clear (transparent),and the solution was subsequently poured into a Teflon bottle. Ten units of sealed both-ended BHFM with a length of 10–15 cm were placed into the bottle and placed inside a steel autoclave. The hydrothermal procedure was conducted at 150 ˚C in an oven (Memmert) for various reaction times (2.5, 5, and 7.5 h) to evaluate the effect of time on the accumulation of TiO_2 on the membrane surface. The, the autoclave container was taken out from the oven. The modified BHFM was taken out and rinsed thoroughly before drying at room temperature.

The TiO_2 nanorods's structure and their dispersion on the external surface of the membrane for BHFM support were studied by using a scanning electron microscope (SEM, Hitachi TM 3000) at several magnifications. TiO_2–BHFM was cut neatly to obtain its crosssection, placed on the metal holder and sputter-coated with gold for 3 min. Energy dispersive X-ray (EDX) analysis was applied to investigate the distribution of elements, whereas atomic force microscope (AFM, SE 100 Park System) was used to observe the surface roughness of the modified BHFM. The existence of the TiO_2 crystalline phase on the external surface of TiO_2–BHFM was determined using an X-ray diffractometer (XRD, Rigaku Smartlab X-Ray diffractometer). The wettability of TiO_2–BHFM was characterised using the contact angle measurement sessile drop method (Dataphysics, OCA 15EC) and deionised water as its contact droplet. Ten different measurement points on the membrane were acquired to determine the average contact angle.

Through cross-flow filtration mode, an ultrafiltration system was used to ascertain water permeability of TiO_2–BHFM with a fibre length of approximately 3–4 cm at a pressure of 3 bar and constant temperature of 25 ˚C. Before any measurement, it was vital to ensure the reading was stable before compacting the TiO_2–BHFM for about 30 min with water used as the feed. The TiO_2–BHFM water absorption was determined according to the following equation:

$$L_p = \frac{\Delta V}{A_m \Delta_t \Delta P} \quad (1)$$

where the permeability of water (L/m^2·h·bar) is represented by L_p, ΔV for the water volume that passed through the membrane (L), A_m represents the effective membrane area (m^2), Δt for the time of permeation (h), and ΔP for the pressure applied (bar). Three measurements were obtained from each membrane sample to determine the average water permeation.

BPA was used as the representative indicator for the photocatalytic efficiency of TiO_2–BHFM on organic contaminants under visible and UV irradiation. Different concentrations of BPA ranged from 30 to 50 ppm were studied. Ten units of TiO_2–BHFM with 10–15 cm length were potted in the membrane reservoir before photocatalytic degradation of BPA using a submerged system.

The submerged system composed of TiO_2–BHFM modules was fitted with a light (LED and UV) as photoreactor system and a beaker witha magnetic bar to homogenise the decaying pollutant. Fig. 1 shows the design of this submerged system. Aluminium foil was used to wrap the glass container to allow the reflecting surface directed to the inner side. The TiO_2–BHFM module was immersed, and suction was applied using a peristaltic pump (Cole Parmer, Masterflex ®L/S) for permeate collection.

Before the photocatalytic reaction, BPA solution was allowed to reach adsorption/desorption equilibrium for about 120 min. Ten millilitres of blank sample was collected before irradiation and treated as the BPA initial concentration (C_0). The solution was then irradiated for 30 min under visible light or UV light. The visible or UV light (36 W) was positioned at the centre of the glass container that was immersed in the synthetic wastewater. UVP UV radiometer evaluated the intensity of light at a distance of 5 cm from the membrane module. Ten millilitres of treated aliquots was extracted within 6 h with 30 min intervals for each sample. The samples were then evaluated for the change in the BPA concentration at 290 nm using high pressure liquid chromatography analysis (Agilent Technologies 1260 Affinity).

3. Results and discussion

3.1. Characterisation of modified BHFM

The hydrothermal method was chosen for the synthesis of TiO_2 particles as it has proven very effective for achieving uniform distribution and giving the best morphological structure of the membrane

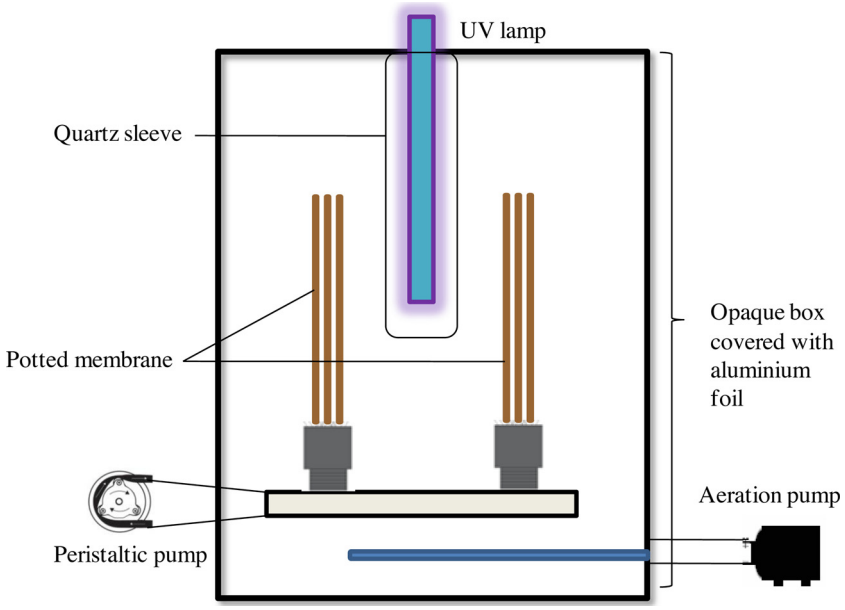

Fig. 1. Schematic of the pilot-scale submerged photocatalytic membrane reactor.

surface. The SEM images of BHFM with 50 wt% loading, sintered 1300 °C for control, 2.5 h, 5.0 h, and 7.5 h are shown in Fig. 2.

The TiO_2 clusters of flowers were successfully embedded on the surface of BHFM. The uniqueness of this structure is commonly due to its specific surface area that is larger than that of the microspheres [19]. The formation of the nanostructures can be varied by controlling the hydrothermal reaction time. As the reaction of hydrothermal was carried out for 2.5 h, the TiO_2 nanorods were not fully formed on the surface of membrane. However, as the reaction time was prolonged to 5 h, flower-like TiO_2 nanostructures were formed and covered about 70 % of the substrate. The TiO_2 nanorods were further grown, and the flower-like structure was obtained when the reaction time was increased to 7.5 h. This result indicates that reaction time determined the morphology of grown nanoparticles on the BHFM surface. This condition yielded a highly uniformed, heterogeneously developed, and widely distributed TiO_2 structure without any aggregation in the substrate. [20].

In terms of pore size of the modified BHFM, longer hydrothermal time reduced the pore size compared to shorter exposure time as shown in Fig. 3. The average membrane pore sizes of TiO_2–BHFM prepared in 2.5 h, 5.0 h, and 7.5 h hydrothermal reaction were of 0.185, 0.059, and 0.043 nm, respectively. Significant pore size shrinkage of 75 % occurred when BHFM was modified within 7.5 h compared to BHFM modified within 2.5 h, which was due to the growing of TiO_2 nanoflower on the surface of the membrane.

The analysis of elemental composition on the outer surface of BHFM was performed using EDX, as shown in Fig. 4. The chemical composition of the modified TiO_2–BHFM is shown in Table 1. Al and Si were present on the external surface of TiO_2–BHFM membrane, while O and Ti were present for the nanoflowers of TiO_2. On the external surface of the membrane, a small quantity of TiO_2 nanoflowers was produced. The TiO_2–BHFM external surface was not entirely dispersed with TiO_2 nanorods, since the elements Ti and O existed on several parts of the membrane external surface, causing the deficiency of TiO_2 layer with a measurable thickness. However, the percentage for TiO_2 nanorods element increased with increment in time from 2.5 h to 5.0 h, indicating the growth in TiO_2 nanoflowers which affected the TiO_2 distribution on the membrane. The distribution for photocatalysts of TiO_2 on the membrane surface should be adequate as it is important to promote the degradation activities on target pollutants through photocatalys is using direct exposure of UV light [21].

Fig. 5 shows the crystalline phases from the modified BHFM through XRD with the increase in TiO_2 peak intensity. The diffraction peak widths of anatase (2 u = 25.48) was narrowed as the time was extended for hydrothermal reaction test. The average crystalline sizes and relative anatase crystallinity are in parallel with the extension in hydrothermal time [22] as it encourages the Ostwald ripening [23] and leads to the development of TiO_2 nanocrystalline particles.

Various hydrothermal reaction time hinders the hydrophilic nature of the altered BHFM. Fig. 6 indicates an improvement contact angle of the BHFM with increase of hydrothermal reaction time, indicating that the surface of the membrane has become coarser with an extended reaction time.

The various effects of reaction time for hydrothermal process on the membrane surface and the BHFM roughness were determined using AFM (Fig. 7). The surface structure of BHFM consists of interconnected, grass-like grains, and irregular peaks due to grain growth during the reaction. The porous structure of the external surface of BHFM with diameter less than 2 nm is defined by high peaks represented by the bright region and deep depressions represented by the dark region that indicate pores and aggregates resembling nodules. Random deposition of TiO_2 was observed when BHFM was exposed to 2.5 h hydrothermal treatment. This finding can be described through the nanorods distribution that demonstrated a non-uniform pattern due to the short reaction time applied. However, when the reaction period was prolonged, several peaks that previously existed disappeared and this significant difference was caused by the reaction time.[24] This finding is parallel with that reported in the previous study conducted by Subramaniam et al. [23] where the coarser surface of the composite membrane was affected by the amount of TiO_2 loading and reaction time.

According to Cao et al. [25], when the membranes were exposed to longer hydrothermal reaction time, the contact angle increased, and their findings show the membrane exhibited a higher contact angle of 84° compared to 78° before the hydrothermal process. The surface modification contributed to the roughness of the membrane as the average surface roughness (Ra value) increased from 1.591 to 2.641 nm after prolonged hydrothermal reaction (from 2.5–7.5 h), increasing the hydrophobicity of the modified membrane and reducing the interaction between water and the membrane surface. TiO_2–BHFM tended to become hydrophobic after hydrothermal treatment, and it could be stipulated that the hydrophilicity of TiO_2–BHFM based on contact angle influences water permeability of membrane [26].

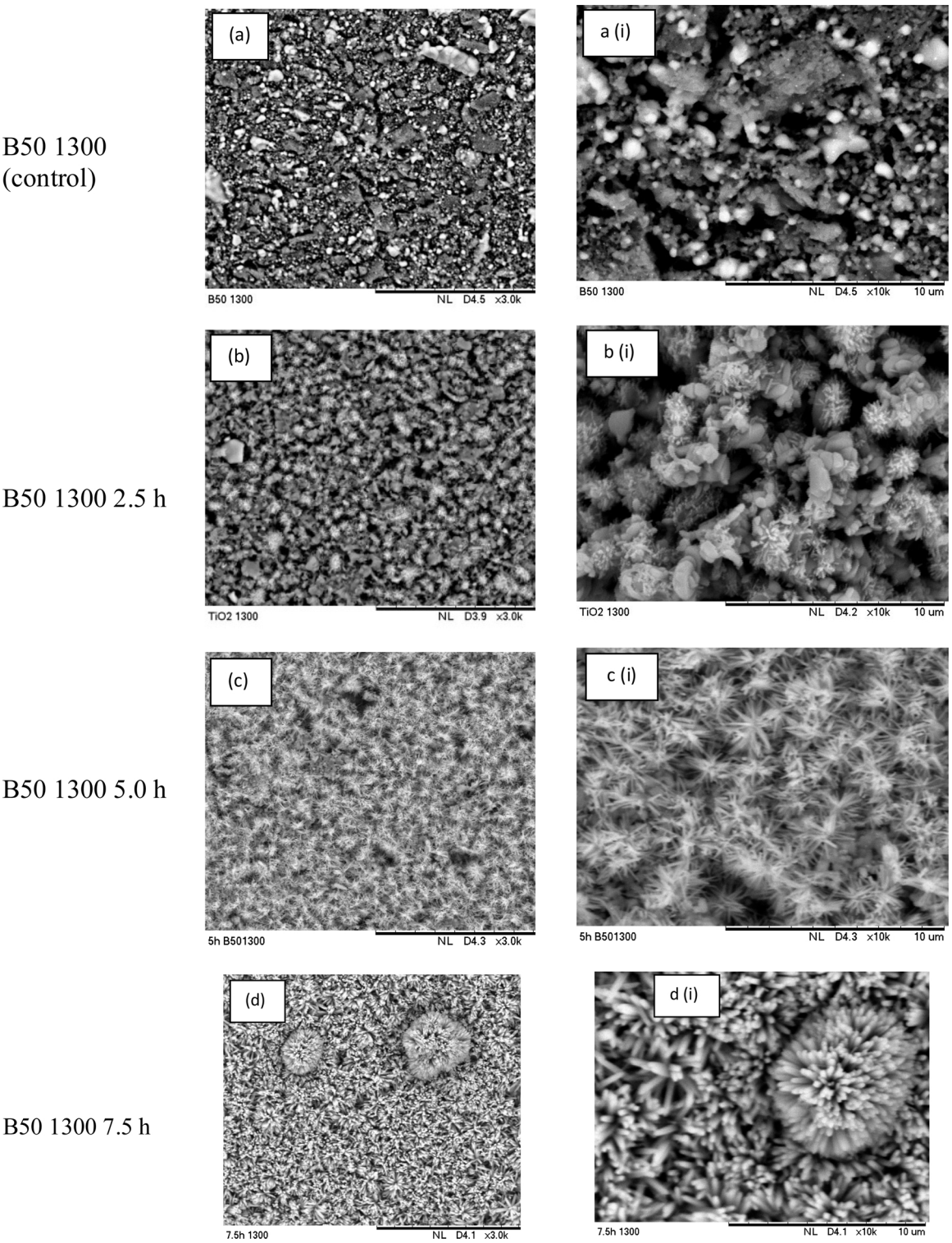

Fig. 2. SEM images of BHFM after hydrothermal process at different durations.

3.2. Water permeation of TiO_2–BHFM

A test of permeability of water towards BHFM was conducted to evaluate the impact of hydrothermal reaction on the permeability of TiO_2–BHFM. Fig. 8 shows the correlation of water permeation to the mechanical strength of the modified BHFM. The increment in the hydrothermal reaction time reduced water permeation of the surface-modified membrane. However, the increment in reaction time increased the mechanical strength. The lowest permeation of 280.42 L/h·m^2·bar was recorded after 7.5 h of hydrothermal reaction compared to 378.79 L/h·m^2·bar for control BHFM. However, longer reaction time improved the water molecules adsorption on the membrane external boosted by the hydroxyl functional groups existence and increase in number on the external surface of BHFM [27]. The FTIR spectra in Fig. 9 support this statement where the band intensities corresponding to the −OH and H−OH− bonds (the FTIR spectra between 3200 and 3550 cm^{-1}) increased after a longer exposure time of hydrothermal treatment. The surface affinity of TiO_2–BHFM also improved, allowing

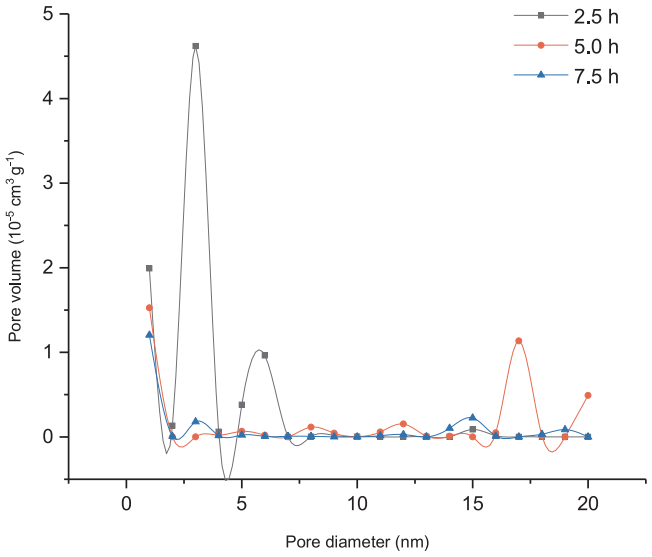

Fig. 3. Average pore size of the modified BHFM based on image J software.

the water molecules to penetrate the membrane.

3.3. Photocatalytic reaction of TiO_2–BHFM on BPA under visible and UV light irradiation

Further experimental works were accomplished to observe the effect of TiO_2 treatment on the membrane using the hydrothermal method. BPA concentrations ranged from 30 to 50 ppm were used, and TiO_2–BHFM of 5.0 h reaction was chosen as the test subject. The rationale of choosing this membrane was based on the obtained physical properties of BHFM with uniform TiO_2 distribution on the membrane surface, less agglomeration, and good water permeability (323.76 L/h·m^2·bar). These properties are required, especially for the photocatalysis work as they affect the performance of the membrane. Prior to the photocatalysis, adsorption/desorption equilibrium experiment was done to ensure that the sorption equilibrium was achieved by observing uniform (constant) sorption triplicate readings and no sorption was detected before photocatalysis as shown in Fig. 10.

Fig. 11 reveals the degradation pattern of 5.0 h TiO_2–BHFM when exposed to visible and UV light irradiation. The degradation of BPA took place efficiently under UV light, and as the concentration of BPA

Table 1
Composition of elements found on BHFM surface after hydrothermal reaction.

Element	Duration of hydrothermal reaction (h)			
	0	2.5	5	7.5
Oxygen	37.93	42.10	41.36	41.68
Aluminium	35.31	16.43	4.54	9.21
Iron	20.03	3.15	0.94	1.77
Silicon	3.45	0.98	0.31	0.28
Titanium	3.19	37.15	46.84	52.70
Zinc	0.08	0.18	0.05	0.23

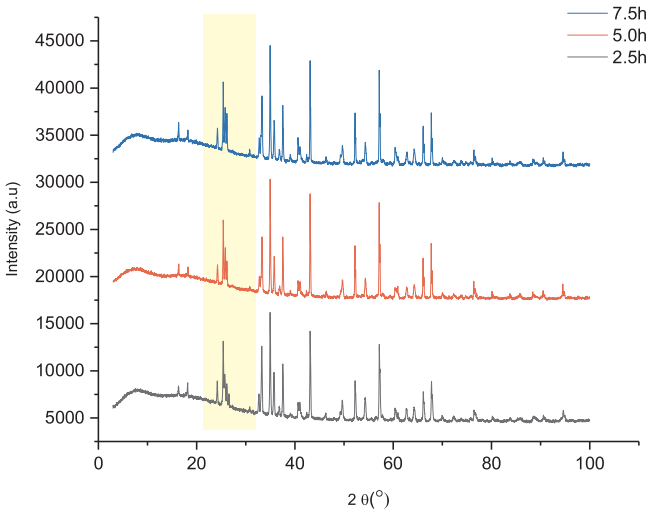

Fig. 5. XRD spectra of modified BHFM at 2.5 h, 5.0 h, and 7.5 h.

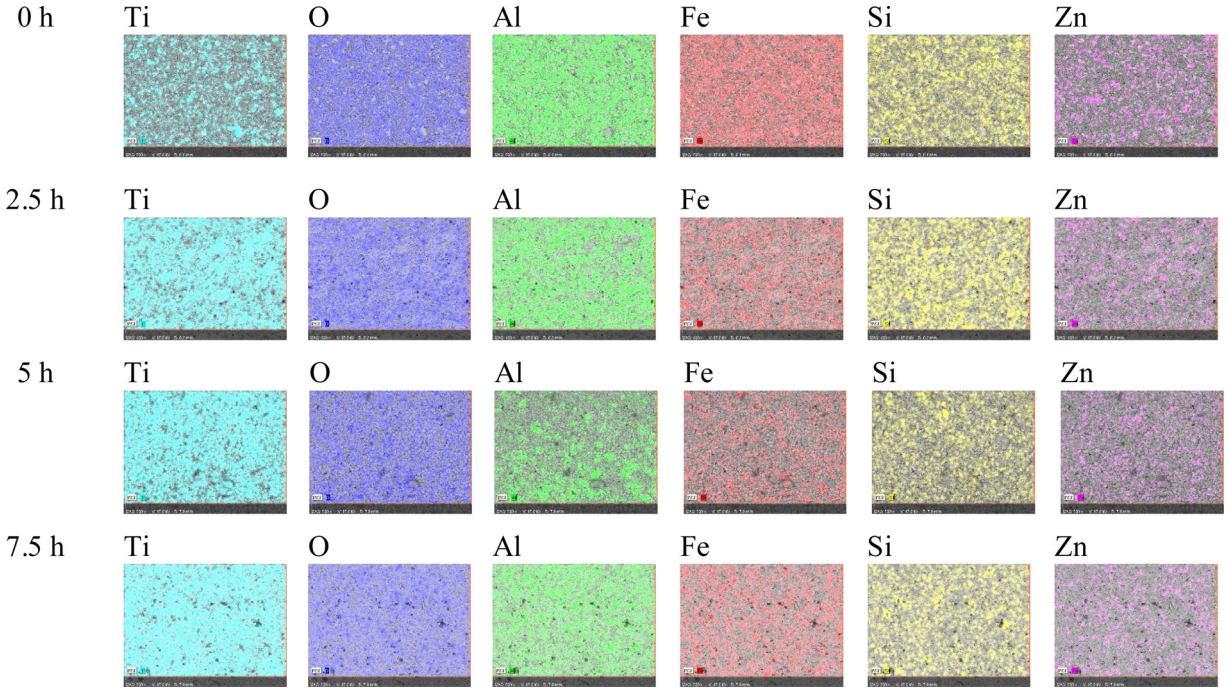

Fig. 4. EDX mapping of different reaction times on BHFM.

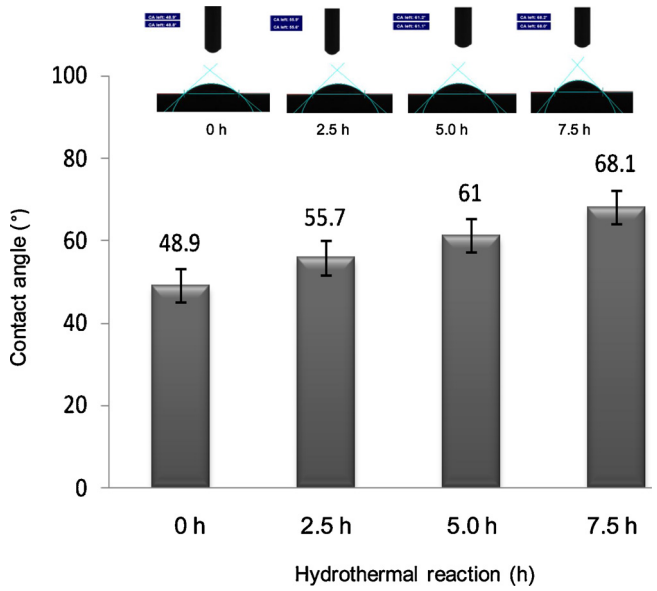

Fig. 6. Contact angles of TiO_2–BHFM prepared at different exposure periods.

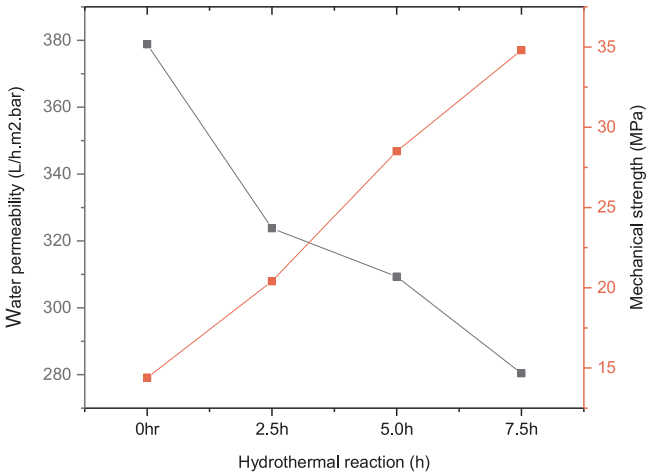

Fig. 8. Water permeation and mechanical strength of TiO_2–BHFM at various hydrothermal reaction times.

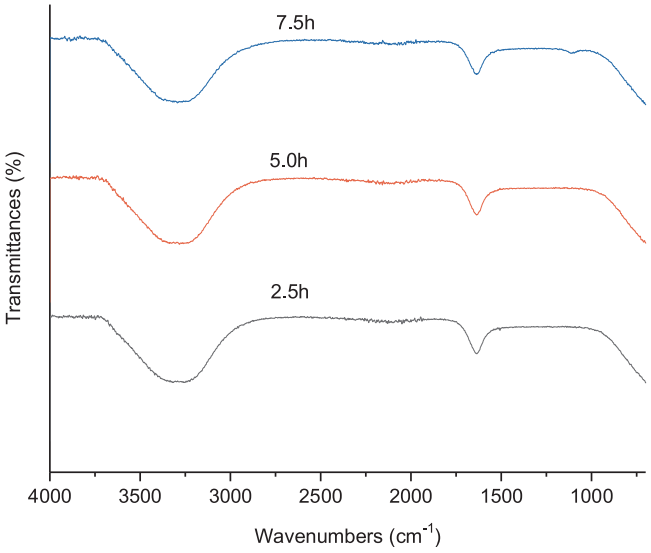

Fig. 9. FTIR spectra of modified BHFM prepared at various hydrothermal times.

decreased, the degradation pattern increased. This result was due to the high amount of available catalyst compared to the amount of contaminants [28]. The highest degradation rate of 78 % was observed using TiO_2–BHFM with 30 ppm BPA under UV light exposure, followed by 40 and 50 ppm BPA. TiO_2exhibits effective response towards UV light due to its large band gap [29], thus this factor would be advantageous.

An additional photocatalytic degradation test was done using 50 ppm BPA to compare and contrast the modified and unmodified BHFM. The rationale of choosing 50 ppm BPA for this section because it was the highest concentration of contaminants used in this study. Fig. 12 shows the degradation pattern of BPA using the unmodified BHFM and TiO_2–BHFM under visible light irradiation. Only 44 % of 50 ppm BPA was removed using unmodified BHFM compared to 52 % removal of BPA by using TiO_2–BHFM and this prove that the modification done in this study was significant to enhance the photocatalytic property of fabricated membrane. The 50 ppm BPA degraded faster under UV light exposure was due to the high recombination site between the catalyst and contaminants. However, as it reached 270 min, the active sites were already occupied, reducing the degradation. The coverage of TiO_2 on the surface changed the property of the surface membrane from visible-light active into UV-light active, reducing the degradation of BPA.

4. Conclusions

BHFM was successfully modified by depositing TiO_2 nanoflowers on the membrane surface using hydrothermal method. Different time periods of hydrothermal exposure gave remarkable effects to the membrane morphology and chemical composition, and these changes enhancedthe degradation rate of BPA at various concentrations. All findings were confirmed using the analyses of SEM analysis, EDX mapping, contact angle, and water permeation. The duration of 5.0 h hydrothermal treatment was considered as the best condition for this modification as the treated BHFM under this condition gave the highest

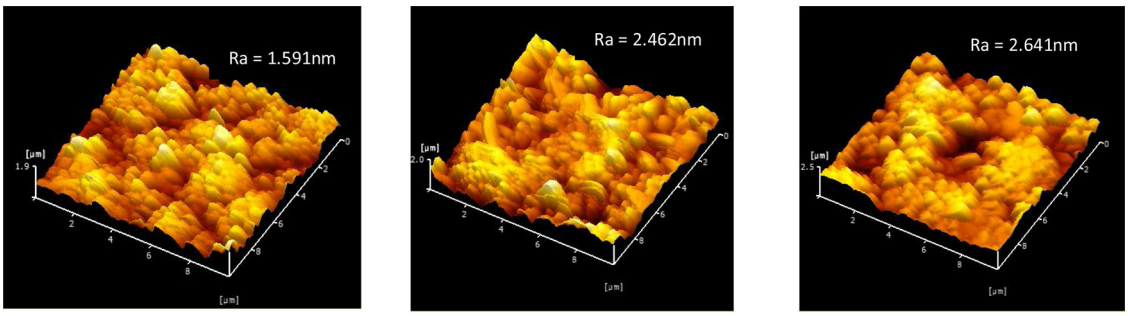

Fig. 7. Surface roughness of TiO_2–BHFM after various reaction times.

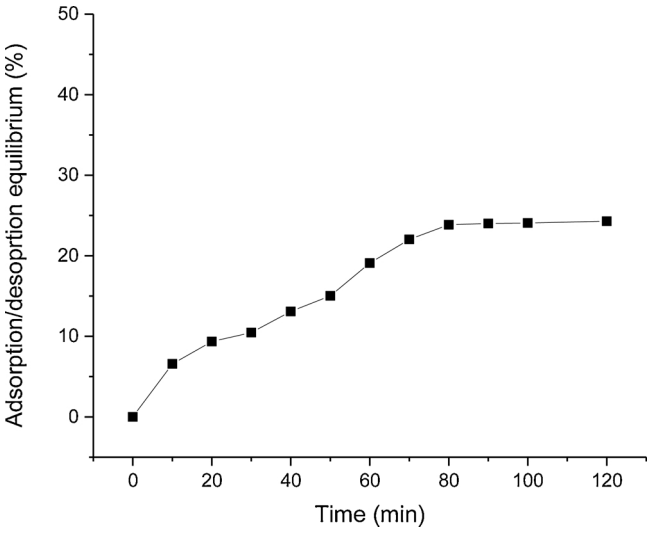

Fig. 10. BPA adsorption/desorption equilibrium curve used in this study.

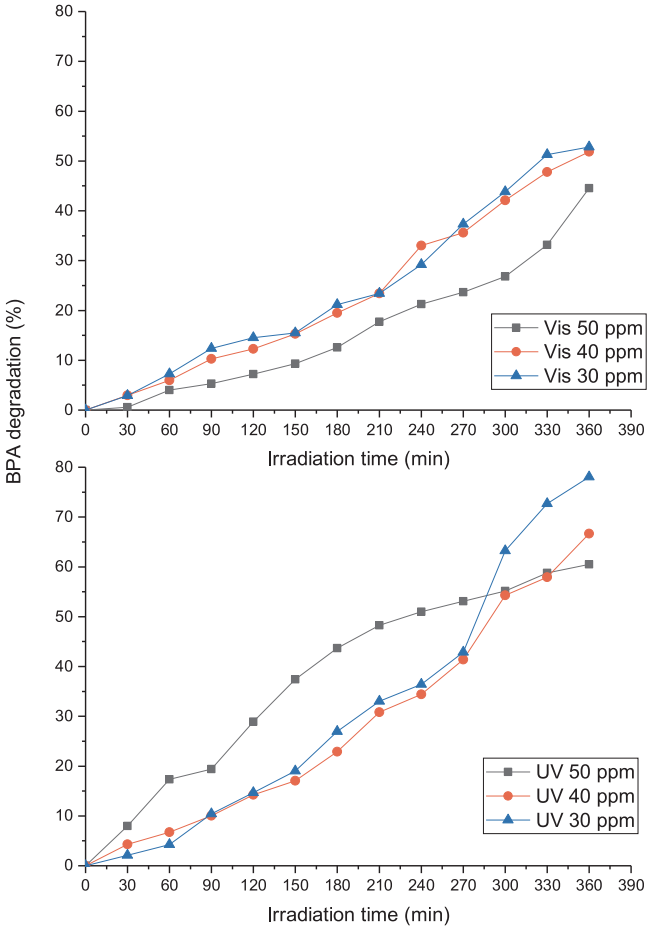

Fig. 11. Degradation of BPA at various concentrations under visible and UV light condition.

removal BPA of 78 % from its initial concentration. The modified BHFM degraded BPA excellently under UV light compared to the unmodified BHFM. However, the unmodified BHFM exhibited better degradation of BPA in 360 min under visible light.

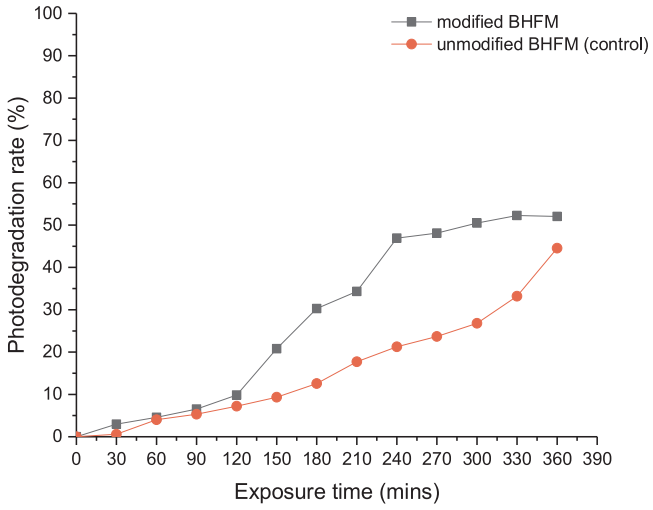

Fig. 12. BPA degradation test using unmodified and modified BHFM.

5. Ethical approval

This article does not contain any studies with human participants or animals performed by any of the authors.

Funding

There is funding source as per stated in the acknowledgement.

Declaration of Competing Interest

The authors declare that they have no conflict of interest.

Acknowledgement

The authors want to express gratitude of financial assistance from the Ministry of Education Malaysia under the Higher Institution Centre of Excellence Scheme (Project Number: R.J090301.7846.4J193) and the Long-Term Research Grant (LRGS) Scheme (Project Number: LRGS (203/PJKIMIA/67215002 & R.J130000.7809.4L895) and Universiti Teknologi Malaysia under the Transdisciplinary Research Grant (Project number: Q.J130000.3509.05G75), Malaysia Research University Network (MRUN) Grant (Project number: R.J130000.7809.4L867), and UTM Grant Award (Project number: R.J130000.7709.5M003).

References

[1] X. Chen, S.S. Mao, Titanium dioxide nanomaterials: synthesis, properties, modifications, and applications, Chem. Rev. 107 (7) (2007) 2891–2959.
[2] H.R. Xia, C. Peng, J. Li, W.T. Sun, G. Ai, L.M. Peng, Large-scale floated single-crystalline TiO2 flower-like films: synthesis details and applications, RSC Adv. 3 (2013) 17668–17671.
[3] H. Choi, E. Stathatos, D.D. Dionysiou, Photocatalytic TiO_2 films and membranes for the development of efficient wastewater treatment and reuse systems, Desalination 202 (2015) 199–206.
[4] D. Reyes-Coronado, G. Rodr´ıguez-Gattorno, M.E. Espinosa-Pesqueira, C. Cab, R. de Coss, G. Oskam, Phase-pure TiO_2nanoparticles:anatase, Brookite and rutile, Nanotechnology 19 (14) (2008) 145605, https://doi.org/10.1088/0957-4484/19/14/145605.
[5] Tsuyoshi Ochiai, Akira Fujishima, Photoelectrochemical properties of TiO_2 photocatalyst and its applications for environmental purification, J. Photochem. Photobiol. 13 (4) (2012) 247–262 Photochemistry Reviews.
[6] Maria D. Hernandez-Alonso, Fernando Fresno, Silvia Suareza, Juan M. Coronado, Development of alternative photocatalysts to TiO2: challenges and opportunities, Energy Environ. Sci. 2 (12) (2009) 1231–1257.
[7] K. Inumaru, M. Murashima, T. Kasahara, S. Yamanaka, Enhanced photocatalytic decomposition of 4-nonylphenol by surface-organografted TiO_2: a combination of molecular selective adsorption and photocatalysis, Appl. Catal. B: Environ. 52 (2004) 275–280.

[8] R.A. Damodar, S.J. You, H.H. Chou, Study the self cleaning, antibacterial and photocatalytic properties of TiO_2 entrapped PVDF membranes, J. Hazard. Mater. 172 (2009) 1321–1328.
[9] Y.F. Lin, K.L. Tung, Y.S. Tzeng, J.H. Chen, K.S. Chang, Rapid atmospheric plasma spray coating preparation and photocatalytic activity of macroporoustitania nanocrystalline membranes, J. Membrane Sci. 389 (2012) 83–90.
[10] H. Dzinun, M.H.D. Othman, A.F. Ismail, M.H. Puteh, M.A. Rahman, J. Jaafar, Morphological study of co-extruded dual-layer hollow fiber membranes incorporated with different TiO_2 loadings, J. Membrane Sci. 479 (2015) 123–131.
[11] B. Liu, E.S. Aydil, Growth of oriented single-crystalline rutile TiO_2 nanorods on transparent conducting substrates for dye-sensitized solar cells, J. Am. Chem. Soc. 131 (2009) 3985–3990.
[12] N.A.M. Nor, J. Jaafar, A.F. Ismail, M.A. Mohamed, M.A. Rahman, M.H.D. Othman, W.J. Lau, N. Yusof, Preparation and performance of PVDF-based nanocomposite membrane consisting of TiO_2 nanofibers for organic pollutant decomposition in wastewater under UV irradiation, Desalination 391 (2016) 89–97.
[13] Z. Zhang, X. Qiao, J. Yu, Microwave selective heating-enhanced reaction rates for mullite preparation from kaolinite, RSC Adv. 4 (2014) 2640–2647.
[14] B.R. Ilic, A.A. Mitrovic, L.R. Milicic, Thermal treatment of kaolin clay to obtain metakaolin, Hem. Ind. 64 (2010) 351–356.
[15] N. Nasuha, S. Ismail, B.H. Hameed, Activated electric arc furnace slag as an efficient and reusable heterogeneous Fenton-like catalyst for the degradation of Reactive Black 5, J. Taiwan Inst. Chem. Eng. 67 (2016) 235–243.
[16] C. Tang, V. Chen, The photocatalytic degradation of reactive black 5 using TiO_2/UV in an annular photoreactor, Water Res. 38 (2004) 2775–2781.
[17] M.N. Chong, Y.J. Cho, P.E. Poh, B. Jin, Evaluation of titanium dioxide photocatalytic technology for the treatment of Reactive Black 5 dye in synthetic and real greywater effluents, J. Clean. Prod. 89 (2015) 196–202.
[18] M.M. Yusoff, M.H. Mamat, M.F. Malek, A.B. Suriani, A. Mohamed, M.K. Ahmad, S.A.H. Alrokayan, H.A. Khan, M. Rusop, Growth of titanium dioxide nanorod arrays through the aqueous chemical route under a novel and facile low-cost method, Mater. Lett. 164 (2016) 294–298.
[19] N.H. Mohtor, M.H.D. Othman, A.F. Ismail, M.A. Rahman, J. Jaafar, N.A. Hashim, Investigation on the effect of sintering temperature on kaolin hollow fibre membrane for dye filtration, Environ. Sci. Pollut. Res. 24 (2017) 15905–15917.
[20] X. Deng, X. Wang, H. Wen, A. Kang, Z. Gui, L. Li, Phase transitions in nanocrystalline barium titanate ceramics prepared by spark plasma sintering, J. Am. Soc. Brew. Chem. 89 (3) (2006) 1059–1064.
[21] A. Harabi, F. Zenikheri, B. Boudaira, F. Bouzerara, A. Guechi, L. Foughali, A new and economic approach to fabricate resistant porous membrane supports using kaolin and $CaCO_3$, J. Eur. Ceram. Soc. 34 (2014) 1329–1340.
[22] R. Sarbatly, Effect of kaolin/PESFratio and sintering temperature on pore size and porosity of the kaolin membrane support, J. Appl. Sci. Faisalabad (Faisalabad) 11 (13) (2011) 2306–2312.
[23] F. Bouzerara, A. Harabi, S. Achour, A. Larbot, Porous ceramic supports for membranes prepared from kaolin and doloma mixtures, J. Eur. Ceram. Soc. 26 (2006) 1663–1671.
[24] R. Subramanian, K.E. Nandini, P.M. Sheila, A.G. Gopalakrishna, K.S.M.S. Raghavarao, M. Nakajima, T. Kimura, T. Maekawa, Membrane processing of used frying oils, J. of the American Chemist' Oil Soc. 77 (3) (2000) 323.
[25] C. Cao, C. Hu, X. Wang, S. Wang, Y. Tian, H. Zhang, UV sensor based on TiO_2 nanorod arrays on FTO thin film, Sens. Actuators B Chem. 156 (1) (2011) 114–119.
[26] M. Zou, F. Xiong, A. Sundaram Ganeshraja, X. Feng, C. Wang, T. Thomas, M. Yang, Visible light photocatalysts (Fe, N):TiO_2 from ammonothermally processed, solvothermal self-assembly derived Fe-TiO2 mesoporous microspheres, Mat. Chem. and Physics 195 (2017) 259–267.
[27] K. Ahmad, C.F. Soon, N. Nafarizal, A.B. Suriani, A. Mohamed, M.H. Mamat, M.F. Malek, M. Shimomura, K. Murakami, Effect of heat treatment to the rutile based dye sensitized solar cell, Optik 127 (2016) 4076–4079.
[28] Y. Hu, D. Li, Y. Zheng, W. Chen, Y. He, Y. Shao, X. Fu, G. Xiao, $BiVO_4$/TiO_2 nanocrystalline heterostructure: a wide spectrum responsive photocatalyst towards the highly efficient decomposition of gaseous benzene, App. Catalysis B: Environment 104 (2011) 30–36.
[29] J. Ng, X. Wang, D.D. Sun, One-pot hydrothermal synthesis of a hierarchical nanofungus-like anatase TiO_2 thin film for photocatalytic oxidation of bisphenol A, App. Catalysis B: Environment 110 (2011) 260–272.